Journal of the Korean Ceramic Society
Vol. 55, No. 5, pp. 440–445, 2018.

https://doi.org/10.4191/kcers.2018.55.5.08

Electrical Transport and Joule Heating of ZrB_2 Network in SiC Matrix

Jung-Hun Kim*, Chang-Yeoul Kim,†, and Sung-Churl Choi*,‡**

**Division of Materials Science and Engineering, Hanyang University, Seoul 04763, Korea*
**Nano-Convergence Material Center, Korea Institute of Ceramic Engineering and Technology, Jinju 52851, Korea*

(Received April 26, 2018; Revised June 20, 2018; Accepted August 22, 2018)

ABSTRACT

To control the electrical properties of a SiC heating element, we sintered SiC-ZrB_2 composites by using the spark plasma sintering method. The addition of ZrB_2 particles with lower electrical conductivity to the SiC matrices with comparatively higher electrical resistivity lowers the electrical resistivities of the composite material. The ZrB_2 particles aggregate to form large particles and 3-1, 3-2, and 3-3 networks, i.e., conduction paths. In our study, about 1-μm-sized ZrB_2 powders start to form the conduction path at about 10 vol.% of addition, namely the threshold volume. The Joule heating experiment shows that 20 vol.% ZrB_2-added SiC heating element has outstanding heating efficiency.

Key words : Spark plasma sintering, SiC, Heating, Electrical resistivity, Percolation

1. Introduction

Silicon carbide (SiC) is a representative non-oxide structural and electrical ceramic material owing to its high thermal and electrical conductivity, high mechanical strength, and high oxidation resistance properties. It is a good ceramic heating element owing to its good electrical conduction and high thermal resistance. Recently, silicon carbide ceramic heaters have been used as the ceramic heating element for three-dimensional chip packages with through-silicon via (TSV) technology and thermo-compression bonding (TCB). However, it is not so easy to control the electrical resistance owing to the difficulty in sintering. Therefore, in this paper, we report on the addition of ZrB_2 to SiC to control the electrical properties. The composition of SiC and ZrB_2 has been studied to investigate the sintering behavior, microstructural development, mechanical and thermal properties, and electrical and heating properties.[1–9] Most previous studies focused on the sintering and mechanical thermal properties with the addition of SiC to ZrB_2 matrices. SiC-ZrB_2 composites were prepared by pressureless sintering, hot-press, or spark plasma sintering (SPS) methods. We adopted the SPS method because it is fast and convenient.

To investigate the properties of diphasic composite materials, percolation and effective media theories were developed. For example, composite materials such as Al_2O_3 precipitates in aluminum and graphite conductive materials in a polymer matrix are widely used in industrial applications as resistors, sensors, and transducers, such as thermistors, piezoresistors, and chemical sensors. Effective media and percolation theories can be used to describe the physical properties, such as electrical resistivity, thermal conductivity, diffusion constants, and permeabilities of diphasic materials. In this paper, we focused on the investigation of electrical conduction with the addition of ZrB_2 to SiC matrices. We adopted ZrB_2 as the high conducting phase in the less conducting material matrix of SiC. In particular, we tried to investigate the connectivity of high conductive ZrB_2 in the less conductive SiC matrix and the percolation theory, and their electrical and Joule heating properties.

†Corresponding author : Chang-Yeoul Kim
E-mail : cykim15@kicet.re.kr
Tel : +82-55-792-2707 Fax : +82-55-792-2730
‡Corresponding author : Sung-Churl Choi
E-mail : cchoi0505@hanyang.ac.kr
Tel : +82-2-2220-0505 Fax : +82-2-2291-6767

2. Experimental Procedure

2.1. Sample preparation

We used silicon carbide powders (β-SiC, 99.8%, 1 μm, Alfa Aesar) and zirconium diboride powders (ZrB_2, 99.5%, 1–2 μm, Alfa Aesar) as raw materials. SiC and ZrB_2 powders were mixed in ethanol with different volume fractions and ball-milled for 36 h using a tungsten carbide ball in a polyethylene jar. The mixture slurry was dried by using rotary evaporator and completely dried in a vacuum oven for 24 h. The fraction of ZrB_2 to SiC was varied from 0% to 50%, in steps of 5%. The samples of SiC/ZrB_2 composites were named as SZ followed by the ZrB_2 fraction. For example, SZ0 indicates 0% of ZrB_2 and SZ50 indicates 50% ZrB_2 in the composites. The dried powders were packed in a graphite mold and sintered by using SPS furnace under 30 MPa. The sintering temperature was increased at 100°C/m up to 1500°C, and 50°C/min from 1500 and 1800°C. The tempera-

ture was maintained at 1800°C for 5 min. The sintering was conducted under a vacuum atmosphere. Samples with dimensions 2 × 2 × 20 mm were grinded and polished. The two edges of the samples were electroded by using silver paste (TEC-PA-051, InkTec) and heat treated at 500°C.

2.2. Characterization

The densities of the sintered samples were measured by the Archimedes method. The relative densities of the samples were calculated by using 3.21 g/cc for SiC and 6.085 g/cc for ZrB_2. The relative density of the samples was 97.86 ± 0.23%. The relative densities and the volume fraction of ZrB_2 are summarized in Table 1. X-ray diffraction (XRD, model D/max-2500/PC, Rigaku, Japan) analysis of the samples was conducted to determine crystal phases, and quantitative analysis was conducted by using the reference intensity ratio values, i.e., 8.10 for ZrB_2 and 3.53 for SiC. Field emission scanning electron microscopy (FE-SEM, JEOL JSM- 7600F, Japan) images were observed, and image analysis was conducted by using the imageJ program. The size distributions and area of ZrB_2 were analyzed. The bulk electrical resistance (R) of the samples were measured by using a multimeter (3250-50, HIOKI, Japan). The electrical resistivity (ρ) was calculated by using the equation, $R = \rho\frac{l}{A}$, where A is the sample area and l is the length. The percolation theory was adopted to interpret the electrical resistivity variations with ZrB_2 volume fraction, where we set the electrical resistivity values as 1.66×10^3 Ω·cm for SiC and 4.0×10^{-5} Ω·cm for ZrB_2. Joule heating of the SiC/ZrB_2 composite resistor was conducted by applying 5 V (D.C. power supply, GP—4303D, EZ, 50V, 3A), and simultaneously measuring the temperature of the sample surface by using a K-type thermometer. The electrical power (P) and energy (U) absorbed in the sample were calculated by the formulas $P = V^2/R$ and U = Pt, respectively, where V is the electrical potential, R is the resistance, and t is time. When the SiC/ZrB_2 resistor samples absorb electrical energy, this energy is dissipated in the form of heat (Q). The heat Q was calculated by $Q = (m_{SiC}c_{SiC} + m_{ZrB2}c_{ZrB2})\Delta T$, where m is the mass of the sample, c is the specific heat capacity, and ΔT is the temperature rise.

Table 1. The ZrB_2 Contents (wt% and vol%) and the Relative Densities of SZ Composite Electrode Sintered at 1800°C

Name	ZrB_2 (wt%)	ZrB_2 (vol%)	Sintering temp. (°C)	Relative Density (%)
SZ0	0	0.0	1800	98.07
SZ5	5	2.7	1800	98.18
SZ10*	10	5.5	1800	97.65
SZ15	15	8.5	1800	97.97
SZ20	20	11.7	1800	97.74
SZ25	25	15.0	1800	97.66
SZ30*	30	18.4	1800	97.23
SZ35	35	22.1	1800	97.80
SZ40	40	26.0	1800	98.31
SZ45	45	30.1	1800	97.56
SZ50*	50	34.5	1800	98.35

* SEM image observation samples

3. Results

The XRD patterns show that the SZ samples comprise ZrB_2 and SiC crystal phases (Fig. 1). The crystal faces of ZrB_2 were identified as (101), (102), (103), and (110), and those for SiC were (001), (100), and (101). When the amount of ZrB_2 was increased, the peak intensities increased, while the intensities of SiC decreased. The XRD results also indicated that there is no reaction between ZrB_2 and SiC, and so, no third crystal phase was found. The volume fraction (V_{ZrB_2}) can be calculated by the relationship between the

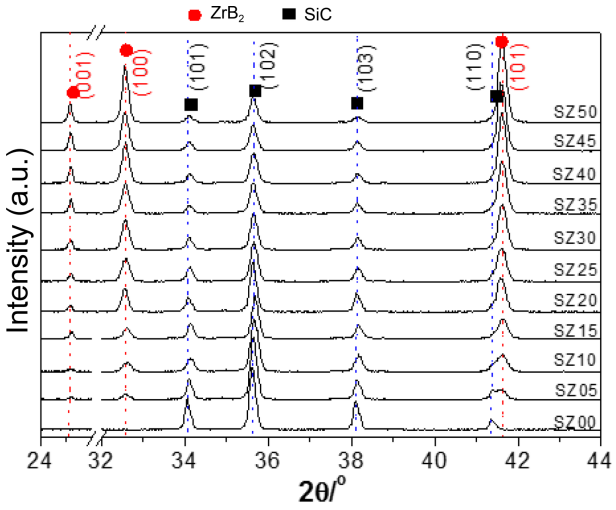

Fig. 1. X-ray diffraction patterns of SiC-ZrB_2 composite electrode between 24° and 44°.

Table 2. Theoretical Volume Percentage and the Measured ZrB_2 Volume Percentage from XRD Peak Area and Intensities (Height)

Sample	ZrB_2 (vol%) Theoretical	ZrB_2 (vol%) Area	ZrB_2 (vol%) Height
SZ0	0.0	0.0	0.0
SZ05	2.7	6.0	4.6
SZ10	5.5	7.2	7.1
SZ15	8.5	14.1	12.1
SZ20	11.7	18.6	16.5
SZ25	15.0	20.7	18.5
SZ30	18.4	24.6	23.2
SZ35	22.1	26.3	26.4
SZ40	26.0	28.3	28.8
SZ45	30.1	30.6	29.4
SZ50	34.5	31.0	32.1

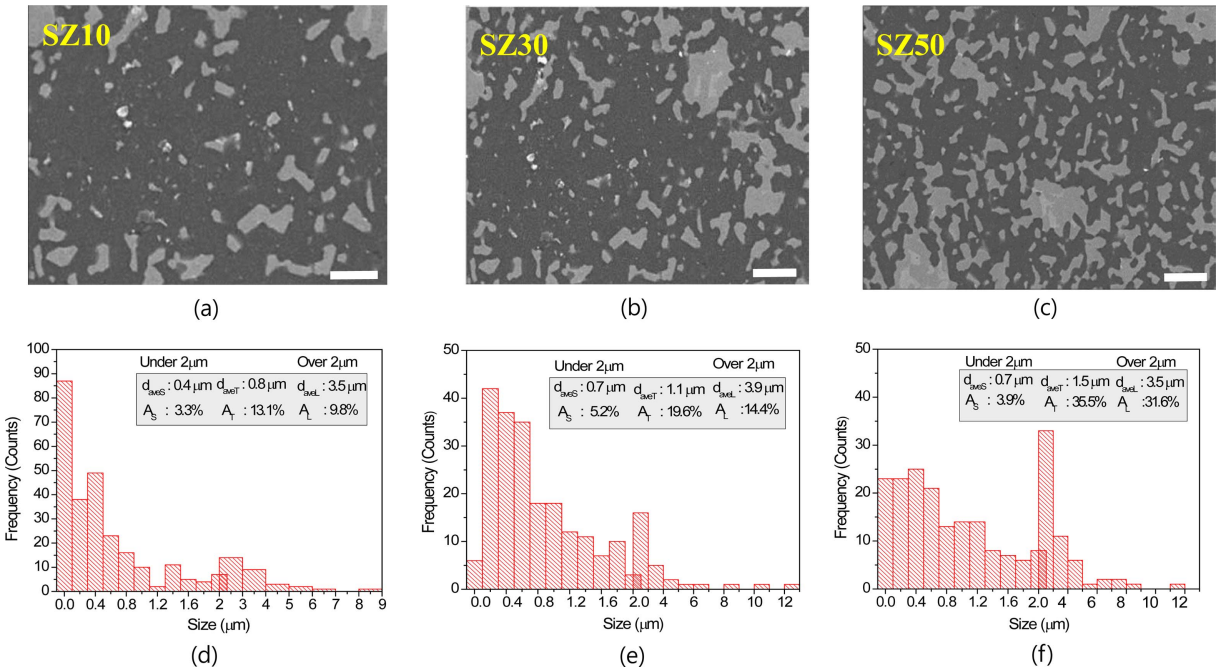

Fig. 2. SEM images of SZ composite electrodes and the ZrB_2 size distributions scattered in the SZ matrices analyzed from SEM images. SZ10 (a) and (d), SZ30 (b) and (e), and SZ 50(c) and (f), respectively. We analyzed the ZrB_2 particles under 2 μm (small) and over 2 μm (large).

structure factor (K_{ZrB_2}) and the linear X-ray absorption coefficient (μ_{ZrB_2}), similar to the following equation:

$$I_{ZrB_2} = \frac{K_{ZrB_2} \times V_{ZrB_2}}{\mu_{ZrB_2}}$$

. However, we do not know the linear X-ray absorption coefficient of ZrB_2, and we therefore adopted the reference-intensity-ratio values against alpha-corundum as 8.1 for ZrB_2 and 3.53 for β-SiC.

As summarized in Table 2, the measured volume fractions are slightly higher than those of theoretical values. This is probably due to the incorrect RIR values for ZrB_2 and SiC crystal phases. However, the XRD analysis results show that the quantities of ZrB_2 phases increased as expected. The volume fractions of ZrB_2 in SiC matrices significantly affect the electrical properties of SZ composite samples. The grain sizes and morphologies of ZrB_2 in SiC matrices also influence the properties of SZ composites. The FE-SEM images of SZ10, SZ30, and SZ50 samples are shown in Fig. 2. In the FE-SEM images, the bright image showed the grains of ZrB_2. The ZrB_2 grains are comprised of small-sized particles less than 2 μm and large-sized particles more than 2 μm. As the volume fraction of ZrB_2 increased, the fraction of small-sized particles decreased, while the fraction of large-sized particles increased. The average particle size of ZrB_2 raw materials is about 1 μm, but in the process of SPS sintering, the grain condensed and grew to form the large-sized particles. The average size of small particles for SZ10 is 0.4 μm and the area fraction is about 3.3%, and the average size of large particles is about 3.5 μm and the area fraction is 9.8%. The total average size of ZrB_2 for SZ10 is about 0.8 μm and 13.1% of area fraction. SZ30 is comprised of small-sized ZrB_2 particles with 0.7 μm and 5.1% of area fraction and 3.9 μm and 14.4%, that is, the total average size of 1.1 μm and the total ZrB_2 fraction of 19.6%. For SZ50,

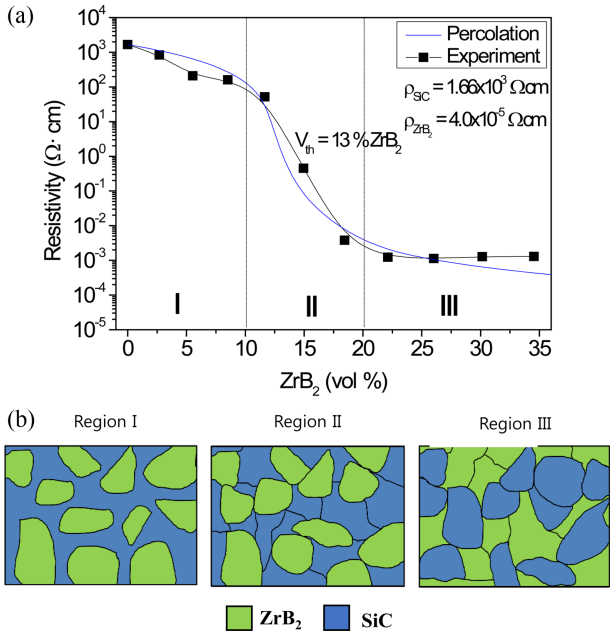

Fig. 3. The electrical resistivity variations (a) and microstructural schematic diagram (b) of ZrB2-SiC composites. Highly conductive ZrB2 fillers are isolated (0-3), one-dimensionally connected (1-3), two-dimensionally connected (2-3) and three-dimensionally connected (3-3) while maintaining the three-dimensional connection of SiC matrices, when the contents of ZrB2 are increased.

the average particle size of small ZrB_2 grains is 0.7 μm with the area fraction of 3.9% and the large particle size was 3.5 μm with the area fraction of 31.6%, and the total average particle size was 1.5 μm with the total area fraction of 35.5%. It indicates that the increase in the ZrB_2 volume fraction infers the aggregation and condensation of the small-sized ZrB_2 particles to form the large-sized particles more than 2 μm, resulting in the decrease in the small-sized particle fraction and the increase in the large particle fraction. The morphology of large-sized particles is irregular, similar to tree leaves with many small branches.

The variations in the electrical resistivities of SZ composites with the volume fractions of ZrB_2 are shown in Fig. 3. The electrical resistivity values are also compared with the percolation simulation data indicated by the blue line. We adopted the following two percolation equations[10,11]: (1) $\rho_m = \rho_h\left(1-\frac{\phi}{\phi_c}\right)^t$ in the region of I and prior half region of II in Fig. 3., and (2) $\sigma_m = \sigma_h\left(1+\frac{f}{f_c}\right)^t$ in the post-half region of II and III in Fig. 3. Here, ρ_m is the electrical resistivity of the SZ composites, ρ_h is the electrical resistivity of SiC bulk sample, ϕ is the ZrB_2 (high conductive) volume fraction, ϕ_c is the critical volume fraction of ZrB_2, σ_m is the electrical conductivities of the SZ composites, σ_h is the electrical conductivity of ZrB_2, f is the SiC (poor conductive) volume fraction, f_c is the critical SiC volume fraction, and t is the exponent between 1.65 and 2.0 (1.7 in this study). We measured the electrical resistivity of the SiC bulk sample[12] to be 1.67×10^3 Ω·cm, but we chose the electrical resistivity of ZrB_2 as 4.0×10^{-5} Ω·cm after referring to the literature.[13] The percolation simulation data is in relatively good agreement with the experimental data when we adopted ϕ_c as 0.13 (13% of ZrB_2 volume fraction), i.e., 0.87 for f_c of SiC volume fraction. The critical volume fraction (ϕ_c) is considered as vP_{cs}, where v is the filling factor of randomly closed packed ZrB_2 and P_{cs} is the critical site percolation probability. The product vP_{cs} = 0.16 can be considered as the critical volume fraction for random packing in three dimensions. The critical volume fraction of ϕ_c varies between 0.01 and 0.6. The value of ϕ_c indicates the average bond number per grain, expressed as

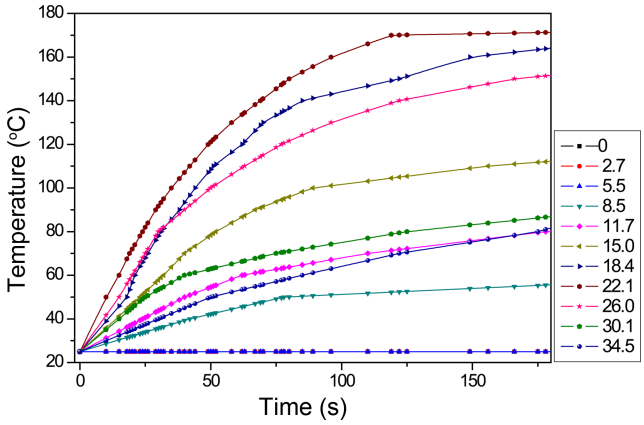

Fig. 4. Electrical resistivity variations in SZ composite electrode with ZrB_2 vol.%, where the electrical resistivities follow the percolation theory with the threshold volume of 13%. The below schematic pictures depict the connections of ZrB_2 dispersed in the matrix in the regions I, II, and III.

ZP_{cb}, where Z is the coordination number and P_{cb} is the critical bond probability. Aharoni[14] gives plausible arguments why the precipitous drop in resistivity as a function of ϕ should commence when the average number of contacts per grain ($\overline{Z}$) is about 1 and cease when it reaches a value of about 2. Our experimental data (ϕ_c = 0.13) is similar to the value 0.16 for random packing of three dimensions.

The Joule heating experimental results of SZ composite resistors are shown in Fig. 4. As mentioned in the experiment section, we conducted the heating experiment in air when we supplied 5 V d.c. electrical potential to the SZ samples and measured the surface temperature by using a K-type thermocouple with time lapse. The applied electrical potential generated electrical current between the two electrodes through the samples and produced heat energy via Joule heating. Until 5.5 vol.% of ZrB_2, there is no change in temperature, and the temperature rise starts for 8.5 vol.%, and the maximum temperature rise was 170°C for 22.1 vol.% SZ sample. It decreased again with more than 26 vol.% of ZrB_2 addition. The resistance variations and temperature rise with the ZrB_2 vol.% are shown in Fig. 5(a).

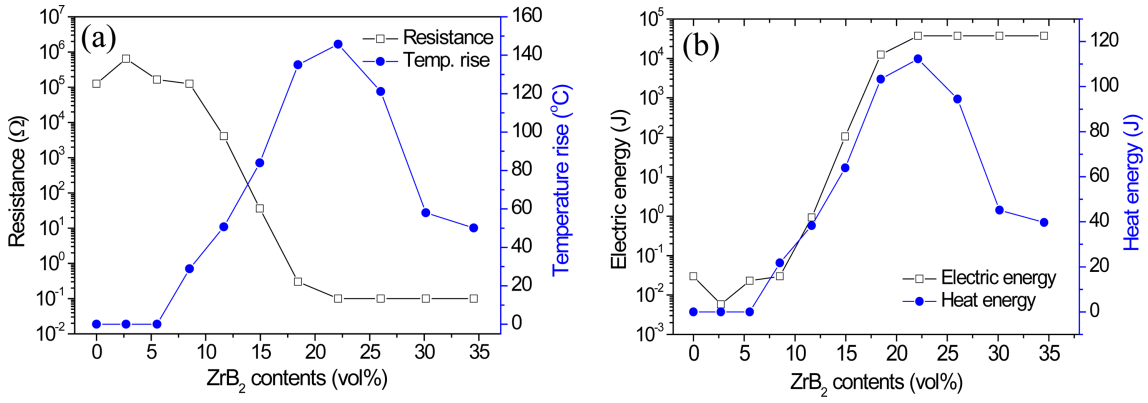

Fig. 5. The temperature rise curves of SZ composite electrodes under the application of 5 V of d.c. electrical potential. The equilibrium temperature was attained for more than 120 s.

Until 5.5 vol.% of ZrB_2, there is no change in the resistance, and the resistance starts to decrease with more than 8 vol.% and is the lowest for 22.1 vol.% of ZrB_2. For more than 22.1 vol.% of ZrB_2 addition, there is no change in the electrical resistance. We guess that the electrical resistance is beyond the limits of our measurement. We can consider the SZ composite resistors for more than 22.1 vol.% of ZrB_2 addition as pure ZrB_2. The electrical energy and heat energy of the SZ samples with the ZrB_2 contents are shown in Fig. 5(b). The electrical energy was calculated based upon the applied electrical voltage and the electrical resistance of the samples. Until 5.5 vol.% of ZrB_2, the electrical energy is very small, of the order of 10^{-2} J, and increased abruptly to 3×10^4 J from 8.5 to 22.1 vol.%. After that, the electrical energy remained constant. However, the heat energy calculated from the heat capacitance and the temperature rise showed a maximum value at 22.1 vol.% of ZrB_2 and then decreased again. For more than 22 vol.% addition, SZ composite resistors are not suitable as Joule heating element. We believe that when more than 22 vol.% of ZrB_2 is added, the SZ composite resistors behave like a metal, allowing easy flow of the electrical current instead of causing Joule heating. However, we did not measure the electrical properties with temperature rise, such as change in electrical resistance with temperature. For example, SiC shows the negative thermistor behavior against temperature. Therefore, we assume that the electrical resistance behavior of SZ composites changes with change in ZrB_2 contents during the Joule heating experiment. To evaluate the effects of the change in electrical resistance with temperature, further research is required. In this research paper, we can say that ZrB_2 addition affects the electrical properties of SZ composite resistor, and this could be interpreted as the percolation theory. In the discussion section, we would like to explain the percolation of ZrB_2 particles via clustering together and the relationship to the Joule heating of the composite resistor. We summarize the electrical and Joule heating properties in Table 3.

4. Discussion

Through this kind of network formation,[11] 0-3 network of ZrB_2 in SiC matrices developed into 1-3, 2-3, and finally 3-3 network formation, as shown in Fig. 6. The green block indicates the ZrB_2 particles and the blue one indicates the SiC particles. When the quantity of ZrB_2 addition into the SiC matrices is increased, the green blocks are linked together in one-dimensional, two-dimensional and three-dimensional directions. When ZrB_2 particles are completely connected together to form three-dimensional networks with the three-dimensional network of SiC particles, the electrical properties are almost similar to those of bulk ZrB_2.

The ZrB_2 particles with an average particle size of 1 μm segregate together to form particles of size smaller than 2 μm and the particles of size larger than 2 μm via a sintering processes (Fig. 6). When the volume fraction of ZrB_2 increases,

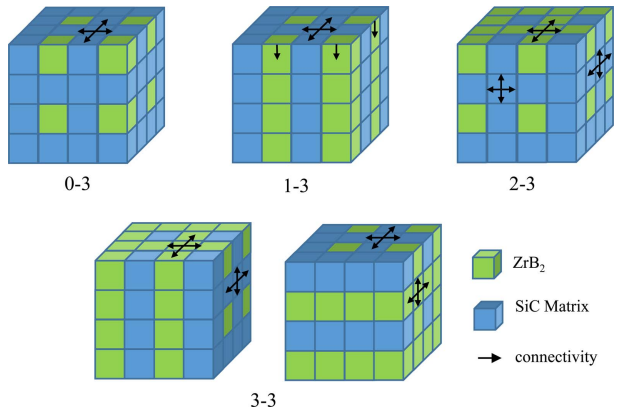

Fig. 6. The variations in resistance and temperature rise (a) and the variations in electrical energy and heat energy with ZrB_2 volume contents (b) of SZ composite electrodes.

Table 3. Densities, Electrical Resistance, Electrical Resistivities, Specific Heat Capacities, and Temperature Rise, Heating and Electrical Energies of SZ Composite Electrode

Name	Density g/cm^3	Resistance Ω	Resistivity Ω·cm	Specific heat capacity J/g°C	Temperature rise °C after 150s	Heat enrgy J	Electrical energy J
SZ0	3.09	126000	1.67×10^3	0.668	0	0.0	0.030
SZ5	3.17	645000	8.36×10^3	0.656	0	0.0	0.006
SZ10*	3.23	164000	2.08×10^3	0.643	0	0.0	0.023
SZ15	3.32	126000	1.59×10^3	0.631	28.9	21.8	0.030
SZ20	3.39	4070	5.16×10^1	0.619	50.7	38.3	0.921
SZ25	3.48	36	4.51×10^{-1}	0.607	84.0	63.9	104.167
SZ30*	3.58	0.3	3.79×10^{-3}	0.594	135.0	103.3	12,500
SZ35	3.68	0.1	1.24×10^{-3}	0.582	145.7	112.3	37,500
SZ40	3.80	0.1	1.13×10^{-3}	0.570	121.1	94.5	37,500
SZ45	3.88	0.1	1.27×10^{-3}	0.557	58.0	45.2	37,500
SZ50*	4.03	0.1	1.30×10^{-3}	0.545	50.1	39.7	37,500

the number of particles smaller than 2 μm decreases and the number of particles larger than 2 μm increases. The small particles cluster together to form about 3.5-μm-sized large particles and the small fraction of the clustered particles are larger than 5 μm. However, the probability of clustering between particles larger than 5 μm is very small, although the probability of particles smaller than 2 μm to form 3.5-μm-sized particles is higher. When the clustering between small particles forms, the connectedness between large particles increases to form an electron transport path, resulting in a decrease in the composites resistors. The aspect ratio of the particles increases with an increase in the ZrB_2 volume fraction. This indicates that the morphologies of ZrB_2 particles are irregular and anisotropic when the ZrB_2 volume fraction increases. The total average particles size also increases from 0.8 μm for SZ10 to 1.5 μm for SZ50. As can be seen in Fig. 3 and Fig. 6, the addition of 10 vol.% of ZrB_2 forms a 3-1 network connection (social class 1, threshold volume) of ZrB_2 clusters and the threshold of electrical resistance drop starts. The addition of 20 vol.% ZrB_2 forms 3-3 networks (social class 2) to result in the similar electrical resistivities of the ZrB_2 sintered material.[12] Based on these results, we draw a conclusion that we can control the electrical resistivities of the composite materials by addition of ZrB_2 in the range of 10 to 20 vol.%.

5. Conclusions

The addition of ZrB_2 particles with the lower electrical conductivity to SiC matrices with the comparatively higher electrical resistivity lowers the electrical resistivities of the composite material. ZrB_2 particles aggregate to form large particles and 3-1, 3-2 and 3-3 networks, that is, conduction paths. In our study, about 1-μm-sized ZrB_2 powders start to form conduction paths at about 10 vol.% of ZrB_2 addition, which is threshold volume. The Joule heating experiment shows that 20 vol.% ZrB_2-added SiC heating element has the best heating efficiency. Based on these results, we conclude that the electrical resistivities of the composite materials can be controlled by addition of ZrB_2 in the range of 10 to 20 vol.%.

REFERENCES

1. S. N. Karlsdottirw and J. W. Halloran, "Oxidation of ZrB_2–SiC: Influence of SiC Content on Solid and Liquid Oxide Phase Formation," *J. Am. Ceram. Soc.*, **92** [2] 481–86 (2009).
2. M. Mallika, S. Roy, K. K. Ray, and R. Mitra, "Effect of SiC Content, Additives and Process Parameters on Densification and Structure–Property Relations of Pressureless Sintered ZrB_2–SiC Composites," *Ceram. Int.,* **39** [3] 2915–32 (2013).
3. S. Kim, J.-M. Chae, S.-M. Lee, Y.-S. Oh, H.-T. Kim, and B.-K. Jang, "Change in Microstructures and Physical Properties of ZrB_2–SiC Ceramics Hot-Pressed with a Variety of SiC Sources," *Ceram. Int.,* **40** [2] 3477–83 (2014).
4. C. Hu, Y. Sakka, H. Tanaka, T. Nishimura, S. Guo, and S. Grasso, "Microstructure and Properties of ZrB_2–SiC Composites Prepared by Spark Plasma Sintering Using $TaSi_2$ as Sintering Additive," *J. Eur. Ceram. Soc.*, **30** [12] 2625–31 (2010).
5. H. Wang, B. Fan, L. Feng, D. Chen, H. Lu, H. Xu, C.-A. Wang, and R. Zhang, "The Fabrication and Mechanical Properties of SiC/ZrB_2 Laminated Ceramic Composite Prepared by Spark Plasma Sintering," *Ceram. Int.,* **38** [6] 5015–22 (2012).
6. J. Han, P. Hu, X. Zhang, S. Meng, and W. Han, "Oxidation-Resistant ZrB_2–SiC Composites at 2200°C," *Compos. Sci. Technol.,* **68** [3–4] 799–806 (2008).
7. J. W. Zimmermann, G. E. Hilmas, and W. G. Fahrenholtz, "Thermophysical Properties of ZrB_2 and ZrB_2–SiC Ceramics," *J. Am. Ceram. Soc.*, **91** [5] 1405–11 (2008).
8. J.-H. Lee, J.-Y. Ju, C.-H. Kim, J.-H. Park, H.-S. Lee, and Y.-D. Shin, "The Development of an Electroconductive SiC-ZrB_2 Composite through Spark Plasma Sintering under Argon Atmosphere," *J. Electr. Eng. Technol.,* **5** [2] 342–51 (2010).
9. J.-Y. Ju, C.-H. Kim, J.-J. Kim, J.-H. Lee, H.-S. Lee, and Y.-D. Shin, "The Development of an Electroconductive SiC-ZrB_2 Ceramic Heater through Spark Plasma Sintering," *J. Electr. Eng. Technol.,* **4** [4] 538–45 (2009).
10. M. B. Isichenko, "Percolation, Statistical Topography, and Transport in Random Media," *Rev. Mod. Phys.,* **64** [4] 961-1039 (1992).
11. D. S. McLachlan, M. Blaszkiewicz, and R. E. Newnham, "Electrical Resistivity of Composites," *J. Am. Ceram. Soc.*, **73** [8] 2187-203 (1990).
12. Y.-W. Kim, K.-Y. Lim, and K. J. Kim, "Electrical Resistivity of Silicon Carbide Ceramics Sintered with 1 wt% Aluminum Nitride and Rare Earth Oxide," *J. Eur. Ceram. Soc.,* **32** [16] 4427–34 (2012).
13. Manab Mallik, Ansu J. Kailath, K. K. Raya, and R. Mitra, "Electrical and Thermophysical Properties of ZrB_2 and HfB_2 Based Composites," *J. Eur. Ceram.Soc.,* **32** [10] 2545–55 (2012).
14. S. M. Aharoni, "Electrical Resistivity of a Composite of Conducting Particles in an Insulating Matrix," *J. Appl. Phys.*, **43** [5] 2463-65 (1972).